Environmental Science & Technology

pubs.acs.org/est

Article

Role of Extracellular Polymeric Substances in Microbial Reduction of Arsenate to Arsenite by *Escherichia coli* and *Bacillus subtilis*

Xinwei Zhou, Fuxing Kang, Xiaolei Qu, Heyun Fu, Pedro J. J. Alvarez, Shu Tao, and Dongqiang Zhu*

Cite This: *Environ. Sci. Technol.* 2020, 54, 6185–6193

Read Online

ACCESS | Metrics & More | Article Recommendations | Supporting Information

ABSTRACT: We show that arsenate can be readily reduced to arsenite on cell surfaces of common bacteria (*E. coli* or *B. subtilis*) or in aqueous dissolved extracellular polymeric substances (EPS) extracted from different microorganisms (*E. coli*, *B. subtilis*, *P. chrysosporium*, *D. gigas*, and a natural biofilm) in the absence of exogenous electron donors. The efficiency of arsenate reduction by *E. coli* after a 7-h incubation was only moderately reduced from 51.3% to 32.7% after knocking out the arsenic resistance genes (*arsB* and *arsC*). Most (>97%) of the reduced arsenite was present outside the bacterial cells, including for the *E. coli* blocked mutant lacking *arsB* and *arsC*. Thus, extracellular processes dominated arsenate reduction. Arsenate reduction was facilitated by removing EPS attached to *E. coli* or *B. subtilis*, which was attributed to enhanced access to reduced extracellular cytochromes. This highlights the role of EPS as a permeability barrier to arsenate reduction. Fourier-transform infrared (FTIR) combined with other chemical analyses implicated some low-molecular weight (<3 kDa) molecules as electron donors (reducing saccharides) and electron transfer mediators (quinones) in arsenate reduction by dissolved EPS alone. These results indicate that EPS act as both reducing agent and permeability barrier for access to reduced biomolecules in bacterial reduction of arsenate.

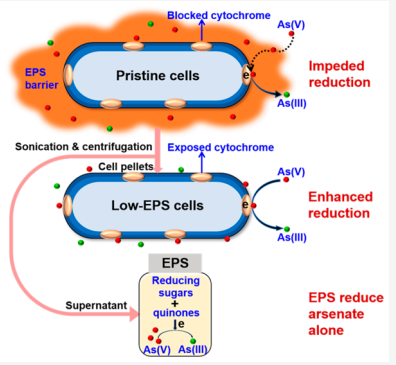

INTRODUCTION

Arsenic (As) is a toxic metalloid element that is widely distributed in surface and subsurface environments at trace levels.[1−3] Concerns about detrimental effects of arsenic on ecological and public health are a major driver to advance understanding of redox processes and mechanisms controlling its environmental fate and toxicity. Arsenic occurs naturally as a variety of species in different valency states (e.g., −3, 0, +3, +5) of which inorganic oxyanions of As(III) and As(V) are the most common forms.[4,5] Arsenate as $H_2AsO_4^-$ or $HAsO_4^{2-}$ exists primarily in oxic environments, while arsenite as $H_3AsO_3^0$ or $H_2AsO_3^-$ exists mostly in anoxic environments.[4,5] Arsenite is generally more toxic and more mobile than arsenate.[1−3] The transformation between arsenate and arsenite is thermodynamically driven by the redox gradient across the environment and involves complex biogeochemical reactions.[6] Not surprisingly, seasonal changes in redox properties, solution chemistry, and biological activities can profoundly affect arsenic cycling in soils, sediments, and groundwater.[4,6,7]

Microorganisms play an essential role in the biogeochemical cycling of arsenic and largely determine the mobilization, transformation, and sequestration of arsenic in the environment.[8−11] It has long been known that certain chemoautotrophic bacteria can use arsenic species as electron donors or electron acceptors for energy generation.[6−8] For instance, bacteria strains (including *Sulfurospirillum barnesii*, *Bacillus selenitireducen*, and *Desulfotomaculum auripigmentum*) isolated from arsenic-rich soils and sediments can grow in laboratory cultures under anoxic conditions with arsenate as the sole electron acceptor, which is consequently reduced to arsenite.[12,13] Not for the sake of harvesting energy for microbial growth, many bacteria possess an arsenic detoxification and resistance function by first reducing less toxic arsenate to more toxic and mobile arsenite within the cell and then expelling it out through efflux pumps.[14,15] This microbial arsenic detoxification process can occur under either oxic or anoxic conditions.[16,17] The most well-studied mechanism of detoxification and resistance is the ArsC system, which is encoded by *ars* operons (*arsRDABC*).[6,18] ArsC reductase encoded by the *arsC* gene mediates the reduction of arsenate to arsenite in the cytoplasm, and the reduced arsenite is excreted via the As(III)-specific transporter ArsB encoded by the *arsB* gene.[6,18] Reduced glutathione and reduced thioredoxin provide the electrons to reduce arsenate inside cells.[6] Although a few studies have addressed the extracellular microbial-induced reduction of arsenate,[11,19,20] only circumstantial evidence exists that this is a feasible process. For example, it has been shown that addition of quinones and riboflavin (both of which can be

Received: February 25, 2020
Revised: April 17, 2020
Accepted: April 21, 2020
Published: April 21, 2020

https://dx.doi.org/10.1021/acs.est.0c01186
Environ. Sci. Technol. 2020, 54, 6185–6193

present in the extracellular matrix) can facilitate the reduction of arsenate by soil microorganisms.[20] Additionally, *in vitro* assays have demonstrated that reduced quinones and semiquinone free radicals as well as reduced glutathione can reduce arsenate to arsenite.[21−23]

Extracellular polymeric substances (EPS) are a major constituent of biofilms (up to 90% in terms of dry weight biomass) and are essential for cell surface attachment and microhabitat formation.[24,25] As an important labile component of the dissolved organic matter (DOM) pool, EPS are deeply involved in biogeochemical cycles of carbon and nutrient elements.[26,27] Also, EPS are known to contain many reducing substances (e.g., proteins and polysaccharide)[25,28,29] and electron transfer mediators (e.g., flavins and quinones).[29−31] However, it remains largely unknown how and to what extent EPS affect the redox-transformation of heavy metal contaminants. In our previous studies, we demonstrated that EPS excreted by common bacteria (*Escherichia coli* and *Bacillus subtilis*) could reduce silver and gold ions (Ag^+, Au^{3+}) to elemental silver and gold nanoparticles (AgNPs, AuNPs) by the contained reducing sugars and thus act as a permeability barrier to these toxic heavy metals.[32,33] These results raise the possibility that EPS may play an important role in affecting the microbial reduction of arsenate.

The main objective of this study was to assess the significance of EPS in microbial reduction of arsenate and discern the active structural components involved in the reaction. Using batch experiments and an array of chemical and spectroscopic analyses combined with gene knockout techniques, we thoroughly investigated the functional components in EPS exfoliated from bacteria and in intact cells responsible for arsenate reduction. This provided valuable insight on the possible impact of microbial EPS on the detoxification and biogeochemical cycling of arsenic in the environment.

MATERIALS AND METHODS

Materials. Standard solutions of sodium arsenate (Na_3AsO_4), arsenic acid (H_3AsO_3), methylarsonic acid (MMA), and dimethylarsinic acid (DMA) of reagent grade were purchased from CNW Technologies GmbH (Germany). Ammonium dihydrophosphate ($NH_4H_2PO_4$, 98.0%) and ammonium nitrate (NH_4NO_3, 96.0%) were also from CNW Technologies GmbH. Chloroauric acid ($HAuCl_4$, > 99.8%) and sodium azide (NaN_3, 99.5%) were from Sigma-Aldrich (St. Louis, MO, USA). Analytical grade nitric acid (HNO_3) (70%) was from Xiya Chemical Reagent (Shandong Province, China). Tryptone, yeast extract, and NaCl of biotechnology grade from Sigma-Aldrich were used to prepare Luria−Bertani (LB) medium for bacterial growth.

Preparation of Microbial Cell Suspensions and Extraction of EPS. The tested bacterial strains were Gram-positive *Bacillus subtilis* (*B. subtilis*, GIM 1.372) and Gram-negative *Escherichia coli* DH5α (*E. coli*, GIM 1.571). The *E. coli* cells were further transformed commercially (Sangon Biotech Co., Ltd., Shanghai, China) by knocking out the plasmid-encoded arsenical resistance operons (*ars*) of the *arsB* gene, the *arsC* gene, and both the *arsB* and *arsC* genes to obtain new strains named Δ*arsB*, Δ*arsC*, and Δ*arsBC*. The bacteria were cultured in 20 mL of LB medium at 37 °C for 12 h, then transferred into 1 L of fresh LB medium, and cultured for another 48 h to reach a stationary phase. The bacteria were separated from LB medium by centrifugation (6000*g* at 4 °C for 10 min), followed by repeated washing with Milli-Q water. The obtained cell pellets were resuspended with Milli-Q water (approximately 3.0×10^{12} cells·L^{-1}) and used for the following extraction of dissolved EPS and kinetic experiments.

Preparation of dissolved EPS from *B. subtilis* or *E. coli* cells was performed using a chemical-free, sonication method as described in our previous studies.[32,33] Briefly, a suspension of bacteria (4.8×10^{12}−8.0×10^{12} cells·L^{-1}) harvested at a stationary phase was sonicated with an intensity of 2.7 W·cm^2 and a frequency of 50 kHz at 4 °C for 15 min to separate EPS from microbial cells and then immediately centrifuged (10000*g* at 4 °C for 20 min) for removing the cells. The supernatant was collected and filtered through a 0.22-μm hydrophilic polytetrafluoroethylene membrane (CNW Technologies GmbH). The obtained filtrate containing dissolved EPS (about 55.0 mgC·L^{-1} on the basis of total organic carbon/TOC) was stored at 4 °C for later use. Cell lysis during the EPS extraction was negligible as indicated by the very low nucleic acid concentration which was measured colorimetrically after reaction with diphenylamine.[33,34] One portion of the bulk aqueous dissolved EPS (28.4 mgC·L^{-1}) extracted from *B. subtilis* was further separated into two different molecular weight (MW) fractions by ultrafiltration using a Centricon-3 membrane with cutoff 3 kDa (Milipore, USA). The obtained low-MW EPS (MW < 3 kDa) and high-MW EPS (MW > 3 kDa) accounted for 63% and 34% of TOC of bulk EPS, respectively. The molecular size distribution of low-MW EPS, high-MW EPS, and bulk EPS was analyzed by high-performance liquid chromatography equipped with a photodiode array detector (Model 1200, Agilent) using an Agilent PL aquagel-OH MIXED-M column (Agilent, USA).

To verify the universality of the reducing capability of EPS, *E. coli*, *Phanerochaete chrysosporium* (*P. chrysosporium*, GIM 3.393), *Desulfovibrio gigas* (*D. gigas*, ATCC19364), and a natural biofilm (mainly *cyanobacteria* and *chlorophyta*) collected from Bailong Lake (32.2° N,119.4° E) in Jiangsu Province, China in the middle of May were investigated as additional microbial sources for EPS preparation. *D. gigas* was grown in a LB medium, and *P. chrysosporium* was grown in a synthetic potato medium (comprising 20% potato juice, 20 g·L^{-1} sucrose, 3 g·L^{-1} KH_2PO_4, 1.5 g·L^{-1} $MgSO_4$, and 10 mg L^{-1} vitamin B1; pH 6.0).[35] The method of EPS extraction was the same as described above.

Reduction of Arsenate in the Presence of Bacteria or EPS. The reduction of arsenate in the presence of *E. coli* or *B. subtilis* cells was examined under two different EPS conditions: without manipulation of EPS (referred to as pristine cells) and with removal of EPS using the above-mentioned sonication/centrifugation method (referred to as low-EPS cells). To initiate the batch reaction experiments, an aqueous stock solution of arsenate was added to a bacterial suspension containing 3.0×10^{12} cells·L^{-1} in 65 mL priorly sterilized polytetrafluoroethylene vials equipped with polytetrafluoroethylene stoppers. The initial concentration of arsenate was 45 μg·L^{-1}. The samples were incubated and shaken by an orbital shaker in the dark at 35 ± 0.5 °C, and aliquots (<0.5 mL) were sampled at desired time intervals (0−9 h). The collected aliquot was treated by the above-mentioned sonication/centrifugation process to help in transferring arsenate and its reaction product (arsenite) into the aqueous phase. The supernatant was withdrawn and stored (referred to as extracellular samples). Selected aliquots of *E. coli* reaction samples were centrifuged (6000*g* at 4 °C for 10 min) without

https://dx.doi.org/10.1021/acs.est.0c01186
Environ. Sci. Technol. 2020, 54, 6185−6193

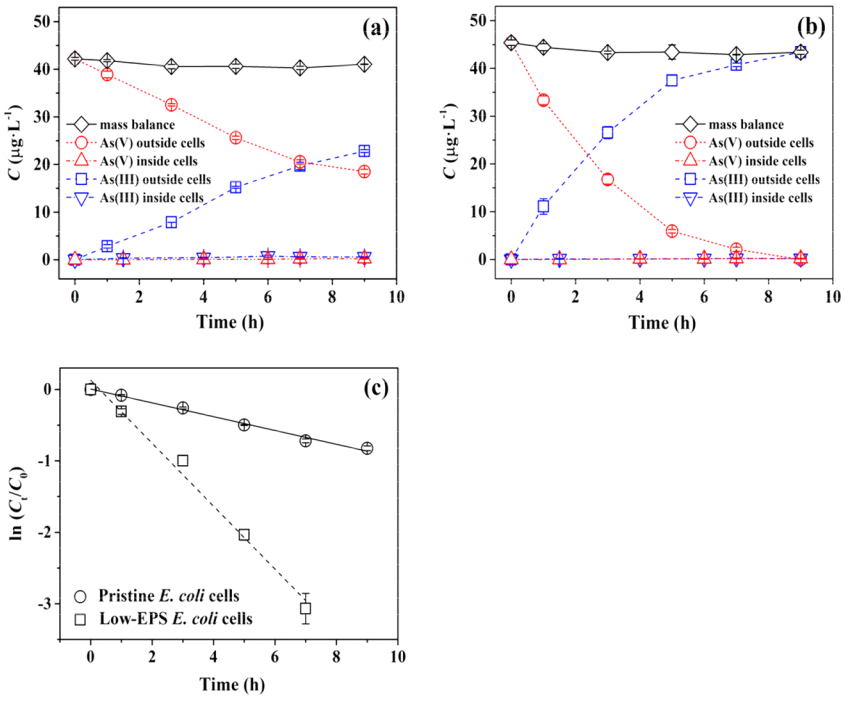

Figure 1. Reduction of arsenate (initially at 45 $\mu g \cdot L^{-1}$) to arsenite in aqueous suspension of *E. coli* (2.8×10^{12} cells$\cdot L^{-1}$) without manipulation of EPS (pristine cells) or with removal of EPS using the sonication/centrifugation method (low-EPS cells). Mass distribution of arsenic species in the presence of pristine *E. coli* cells (a) or low-EPS *E. coli* cells (b). Pseudo-first-order kinetics of reduction of arsenate plotted as $\ln(C_t/C_0)$ against time for pristine *E. coli* cells and low-EPS *E. coli* cells (c). Error bars represent standard deviations calculated from triplicate samples.

sonication, and the supernatants were collected (referred to as medium samples). To test intracellular uptake and reduction of arsenate, selected cell pellets after removal of EPS were resuspended with Milli-Q water and disrupted by highly intensive focused ultrasound (HIFU) (Φ2, Scientz, China) with an intensity of 450 W·cm^2 and a frequency of 24 kHz at 0 °C for 5 min. After centrifugation (12000*g* at 4 °C for 20 min), the supernatant containing the cell lysate was collected and stored (referred to as intracellular samples). A separate set of experiments was performed to assess the effect of sodium azide (7.7 mM) (a cytochrome inhibitor)[36,37] on arsenate reduction by *E. coli* cells or *B. subtilis* cells. Triplicate samples were run for each time point in batch reaction experiments. The pH of bacterial suspensions was 7.3 ± 0.2 at the end of the experiments.

Meanwhile, the kinetics of arsenate reduction in the presence of EPS extracted from different microorganisms (*B. subtilis*, *E. coli*, *P. chrysosporium*, *D. gigas*, and a natural biofilm) was examined by similar sets of experiments, except that the operation was conducted in a glovebox filled with high-purity nitrogen for eliminating oxygen. The batch reaction solution containing EPS (about 55.0 mgC$\cdot L^{-1}$) was purged with nitrogen to remove dissolved oxygen prior to spiking of arsenate (initially at 10.0 $\mu g \cdot L^{-1}$). In addition, the fractionalized low-MW EPS and high-MW EPS separated from the bulk *B. subtilis* EPS were also tested. Separate sets of experiments were run to assess the effects of juglone (5.7 μM) (an electron transfer mediator), dissolved oxygen (without N_2 purging), and gold ion (Au^{3+}, 25 μM) (a consumer of reducing agents such as hemiacetals)[33] on arsenate reduction by EPS. Triplicate samples were run for each time point in batch reaction experiments. The pH of EPS solutions was measured to be 7.5 ± 0.2 at the end of the experiments.

Determination of Arsenic Species. The total arsenic concentration of the collected samples was determined by inductively coupled plasma-mass spectrometry (ICP-MS) NexION 300X (PerkinElmer, USA) using a method similar to that in previous studies.[38] The samples were further analyzed by high-performance liquid chromatography (HPLC)-ICP-MS using a PRP-100X 10-μm anion-exchange column (Hamilton, Switzerland) to determine concentrations of different arsenic species.[38] The mobile phase consisted of 8.0 mM $NH_4H_2PO_4$ and 8.0 mM NH_4NO_3, adjusted to pH 6.2 using ammonia. Isocratic elution was run at 25 °C with a flow rate of 1.2 mL$\cdot$min^{-1}. Identifications of arsenic species (arsenite, arsenate, DMA, and MMA) were verified by the retention times of the corresponding standard compounds. Their concentrations were measured based on calibration curves prepared by standard compounds.

Structural Characterization of EPS. *B. subtilis* EPS (28.4 mgC$\cdot L^{-1}$) and *E. coli* EPS (32.3 mgC$\cdot L^{-1}$) with and without reaction with arsenate (40 $\mu g \cdot L^{-1}$) were placed at −70 °C for 72 h, and then the frozen EPS were completely dried to a powder by freeze-drying. The dried EPS and KBr were mixed by a ratio of 1:100 and homogenized in an agate grinder. About 150 mg of the mixture was compressed and analyzed on a Nicolet NEXUS870 FTIR spectrometer (USA) with a spectral range of 4000−400 cm^{-1}, 32 scans, and a resolution of 4 cm^{-1}. Elemental compositions of the freeze-dried pristine EPS were determined by a Vario MICRO cube (Elementar, Germany). The excitation−emission matrix (EEM) fluorescence spectra of *B. subtilis* EPS (10 mgC$\cdot L^{-1}$) were recorded on a Shimadzu F-7000 fluorometer (Japan) with an excitation wavelength range of 230−500 nm and an emission wavelength range of 270−700 nm.[39]

The consumption of hemiacetal groups in EPS extracted from different microorganisms resulting from reaction with

https://dx.doi.org/10.1021/acs.est.0c01186
Environ. Sci. Technol. 2020, 54, 6185−6193

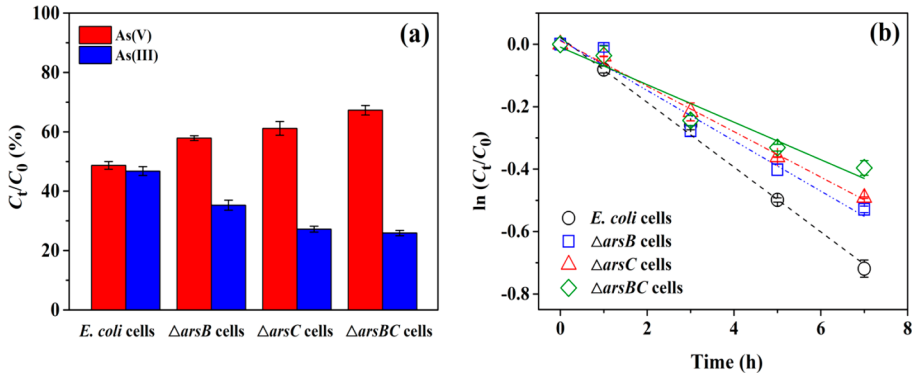

Figure 2. Reduction of arsenate (initially at 45 $\mu g \cdot L^{-1}$) to arsenite in aqueous suspension of wild-type *E. coli* and blocked mutants (Δ*arsB* cells, Δ*arsC* cells, and Δ*arsBC* cells) (all in 2.8×10^{12} cells·L^{-1}). Ratios of concentrations (C_t) of residual arsenate and arsenite (product) at the end of the reaction (7 h) to the initial concentration (C_0) of arsenate (a) and pseudo-first-order kinetics of reduction of arsenate plotted as $\ln(C_t/C_0)$ against time (b). Error bars represent standard deviations calculated from triplicate samples.

arsenate was determined by Tollens' reagent.[33,40] Briefly, Tollens' reagent ($Ag(NH_3)_2OH$) was freshly prepared by gradually dropping aqueous NaOH solution (5%, w/v) into a clean glass test tube containing 1 mL of aqueous $AgNO_3$ solution (2%, w/v) to form precipitates and followed by dropping aqueous ammonia solution (2%, w/v) until the precipitate just dissolved. Four different EPS (64−94 mg·L^{-1}), each extracted from a suspension of individual microbial species (*E. coli*, *B. subtilis*, *D. gigas*, or *P. chrysosporium*), were reacted with arsenate (40 $\mu g \cdot L^{-1}$) for 72 h under the same conditions as described earlier. Then 10 mL of neat EPS solution or arsenate-reacted EPS solution was mixed with 1 mL of Tollens' reagent, respectively. The mixtures were water bathed for 10 min at 50 °C, followed by adjusting pH to 4.0 in order to turn the unreacted $Ag(NH_3)_2OH$ into Ag^+. The produced Ag^+ was titrated using an autotitrator (WDDY-2008J, Datang, China) equipped with a silver ion-selectivity electrode (Pag/S-1-01, INESA, China) and a mercurous sulfate reference electrode (C-K_2SO_4-1, INESA, China). The titration was performed using 0.1 mmol·L^{-1}NaCl with a speed of 10 μL per 20 s at 30 °C and 150 rpm magnetic stirring. The content of hemiacetal groups (aldehyde equivalents) in EPS was calculated from the amount of elemental silver (Ag^0) produced from the Tollens' reagent. The consumption of hemiacetal groups in EPS due to reaction with arsenate was calculated by subtracting the content of aldehyde equivalents in arsenate-reacted EPS from that in neat EPS. Duplicate samples were run for each tested EPS.

RESULTS AND DISCUSSION

Arsenate Reduction by Bacterial Suspension. Figure 1a,b displays the loss of arsenate (initially at 45 $\mu g \cdot L^{-1}$) and the formation of arsenite as a function of time (0−9 h) with the presence of *E. coli* cells without manipulation of EPS (pristine cells) or with removal of EPS by sonication/centrifugation (low-EPS cells). The kinetics of arsenate reduction was best described by the pseudo-first-order model ($R^2 > 0.985$), plotted as the natural logarithm ratio of arsenate concentration at a given time (C_t) to the initial arsenate concentration (C_0) against time (Figure 1c). The respective data of arsenate reduction in the presence of pristine/low-EPS cells of *B. subtilis* are displayed in Figure S1a−c (Supporting Information). The observed pseudo-first-order rate constants (k_{obs}, h^{-1}) for these bacteria are summarized in Table S1. For all tested cells, arsenite was the only reduction product detected, while organic arsenic species (MMA and DMA) were not detected during the reaction process (detection limit about 0.5 $\mu g \cdot L^{-1}$). Moreover, most of the total arsenic was found outside of the cells (>96% measured with the medium samples; >97% measured with the extracellular samples), and the presence of arsenic inside the cells was negligible (<2%, measured with the intracellular samples). The recovery of total arsenic (e.g., mass balance) ranged from 92.4% to 99.2%.

Arsenate was readily reduced by pristine cells of *E. coli* and *B. subtilis*, and the reduction efficiency (defined as the ratio of the reduced arsenate to the initial arsenate added at the end of the 9-h reaction) was 56.1% and 35.1%, respectively. Apparently, *E. coli* exhibited stronger reducing ability than *B. subtilis*. The reduction kinetics was pronouncedly accelerated by removing EPS attached to cells. For low-EPS cells of *E. coli* and *B. subtilis*, the reduction efficiency was 100% and 82.8%, respectively. With the removal of EPS, the k_{obs} was increased by 3.5-fold for *E. coli* cells and by 2.9-fold for *B. subtilis* cells. We previously showed that reduction of Au^{3+} to AuNPs by *E. coli* cells was suppressed by the removal of EPS from cells, which was attributed to the loss of reducing agents (reducing saccharides) in EPS.[33] These contrasting results (Figure 1) indicate that EPS played different roles in the reduction of arsenate versus Au^{3+}, likely due to two different characteristics of these ions. First, Au^{3+} is much easier to reduce than arsenate. At pH 7, the standard electrode potential of half reaction is 1.498 V for Au^{3+}/Au^0 and is 0.135 V for $H_2AsO_4^-/H_3AsO_3$.[6,21,41] Second, Au^{3+} is a cation, whereas arsenate is an anion (dominated by $H_2AsO_4^-$ and $HAsO_4^{2-}$ at pH 7.5). Bacterial EPS are enriched in negatively charged functional groups (mainly phosphates and deprotonated carboxyls).[24,25] Thus, the electrostatic attraction force would facilitate transport of Au^{3+} through EPS, whereas electrostatic repulsion would hinder diffusion of arsenate. Thus, EPS acted as a transport barrier and suppressed bacterial reduction of arsenate.

It is well-known that some bacteria, including *E. coil* and *B. subtilis*, can reduce arsenate to arsenite intracellularly and then expel arsenite outside cells.[18,42] This arsenate reducing capability is probably inherited from archaebacteria that used to exist in an arsenic-rich paleoenvironment and thus developed the functional genes for arsenic respiration and resistance.[6,18] Arsenate reductase (ArsC) in the cytoplasm of *E. coli* and *B. subtilis* cells can catalyze the reduction of arsenate to arsenite, whereas membrane protein ArsB acts as a specific

https://dx.doi.org/10.1021/acs.est.0c01186
Environ. Sci. Technol. 2020, 54, 6185−6193

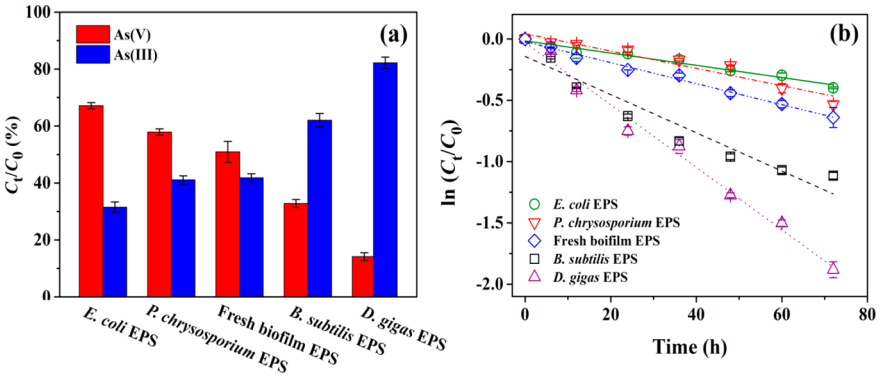

Figure 3. Reduction of arsenate (initially at 10 $\mu g \cdot L^{-1}$) in aqueous dissolved EPS (approximately 55 $mgC \cdot L^{-1}$) extracted from different microorganisms (*E. coli, B. subtilis, D. gigas, P. chrysosporium*, and natural biofilm). Ratios of concentrations (C_t) of residual arsenate and arsenite (product) at the end of the reaction (72 h) to the initial concentration (C_0) of arsenate (a) and pseudo-first-order kinetics of reduction of arsenate plotted as $\ln(C_t/C_0)$ against time (b). Error bars represent standard deviations calculated from triplicate samples.

efflux pump extrudes arsenite from the cytoplasm.[6,42] Figure 2 compares the reduction efficiency and the pseudo-first-order reaction kinetics of arsenate reduction between *E. coli* and its blocked mutants (Δ*arsB*, Δ*arsC*, and Δ*arsBC*). Their respective k_{obs} values are shown in Table S1. After the 7-h reaction, the reduction efficiency followed the order of wild-type *E. coli* > Δ*arsB* > Δ*arsC* > Δ*arsBC*. Compared with wild-type *E. coli*, the reduction efficiency decreased by 17.9%, 24.4%, and 36.3% for Δ*arsB*, Δ*arsC*, and Δ*arsBC*, respectively, indicating that arsenate reduction by *E. coli* blocked mutants was impeded but not stopped. Notably, similar to wild-type *E. coli* cells, most (>97%) total arsenic was present outside the mutant cells. Although a few studies reported that the physiological role of the chromosomal *ars* operon appeared to confer low-level arsenic resistance,[43] we postulate that, in addition to intracellular pathways, there are extracellular pathways involved in arsenate reduction by *E. coli* cells.

Arsenate Reduction by EPS. Figure 3 displays the reduction efficiency and the pseudo-first-order reaction kinetics for arsenate reduction by the five different aqueous dissolved EPS. The dissimilar microorganisms used to prepare EPS represent a wide diversity, including *E. coli* (Gram-negative facultative bacterium), *B. subtilis* (Gram-positive bacterium), *P. chrysosporium* (aerobic fungus), *D. gigas* (anaerobic bacterium), and natural biofilm (mainly *cyanobacteria* and *chlorophyta*). Similar to bacterial suspensions, arsenite was the only product identified in arsenate reduction by EPS. A very good mass balance (>98.9%) was achieved during the reduction of arsenate by *B. subtilis* EPS (Figure S2). The reducing capability of EPS seemed to be much lower when compared with bacterial cells. Given a reaction time of 72 h, the reduction efficiency of arsenate was 32.9%, 67.2%, 85.9%, 42.1%, and 49.1% for EPS extracted from *E. coli, B. subtilis, P. chrysosporium, D. gigas*, and natural biofilm, respectively. Their respective k_{obs} values ranged from $(5.0 \pm 0.4) \times 10^{-3}$ h^{-1} to $(2.5 \pm 0.1) \times 10^{-2}$ h^{-1} (Table S2). Among the tested EPS samples, *D. gigas* EPS showed the highest reducing capability, whereas *E. coli* EPS showed the lowest reducing capability. Contrary to bacterial suspensions, *E. coli* EPS showed much lower reduction efficiency than *B. subtilis* EPS, suggesting that bacterial cells and their EPS are not positively related in terms of arsenate reducing capability. The reduction efficiency of arsenate by different EPS extracted from *E. coli* and its blocked mutants (Δ*arsB*, Δ*arsC*, and Δ*arsBC*) is compared in Figure S3. Compared with EPS from wild-type *E. coli*, the reduction efficiency was only slightly or moderately decreased by 4.3%, 15.9%, and 23.0% for EPS from Δ*arsB*, Δ*arsC*, and Δ*arsBC*, respectively. These results imply the universal capability of microbial EPS for reducing arsenate, and that this capability is not very dependent on the specific proteins/peptides encoded by the arsenic resistance genes.

Identification of EPS Reducing Agents. To reveal the structural components in EPS responsible for arsenate reduction, the FTIR spectra of the pristine EPS from *E. coli* and *B. subtilis* cells were compared with those of the corresponding EPS after reaction with arsenate (Figure 4). The two pristine EPS showed very close spectral patterns, reflecting their similar functional groups. Several distinctive spectral bands were identified for the two pristine EPS, including 1636 cm^{-1} (Amide I), 1400 cm^{-1} (carboxylic groups), 1245−1240 cm^{-1} (Amide III), 1110−1040 cm^{-1}

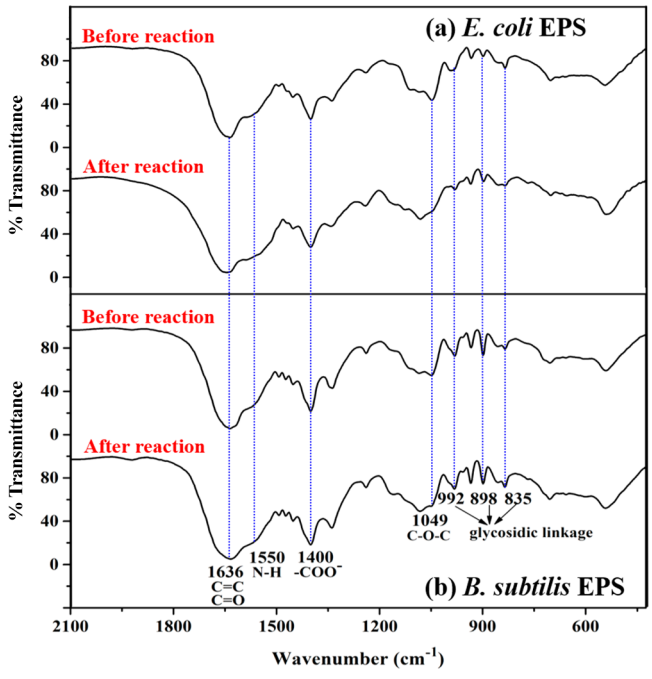

Figure 4. Fourier-transform infrared (FTIR) spectra of EPS before and after reaction with arsenate (initially at 40 $\mu g \cdot L^{-1}$). (a) *E. coli* EPS (initially at 32.3 $mgC \cdot L^{-1}$). (b) *B. subtilis* EPS (initially 28.4 mg $C \cdot L^{-1}$).

https://dx.doi.org/10.1021/acs.est.0c01186
Environ. Sci. Technol. 2020, 54, 6185−6193

(carbohydrates), and 900−600 cm^{-1} (fingerprint region).[39,44] After reaction with arsenate, the peaks at 1049 cm^{-1} (polysaccharide C−O−C), 992 cm^{-1} (glycosidic linkage), 898 cm^{-1} (glycosidic linkage), and 835 cm^{-1}(glycosidic linkage)[44−46] became weaker or even disappeared, indicating that the reducing saccharides were involved in the reaction. In contrast, the peaks originated from peptide amide I (1636 cm^{-1}) and amide II (1550 cm^{-1})[39,44] were not much altered. Thiol-bearing peptides or proteins were reported to reduce arsenate.[23] However, thiol-induced reduction was ruled out as the main cause for arsenate reduction by EPS in this study, because the arsenate reducing capability of *B. subtilis* EPS was much higher than that of *E. coli* EPS despite the lower sulfur content of the former (see elemental composition results in Table S3). To further assess the importance of reducing saccharides in arsenate reduction, we investigated the relationship between the reduction efficiency of arsenate and the consumption of reducing sugar content (determined as aldehyde equivalent, $\mu mol \cdot g^{-1}$) resulting from reaction with arsenate for the four EPS extracted from the pure-culture microorganisms (Figure 5). The arsenate reducing capability of EPS was positively related (but not linearly correlated) to the reducing sugar content consumed, confirming the key role of reducing saccharides in arsenate reduction. Similarly, previous studies have proposed that the reducing saccharides in EPS act as an important reducing agent to facilitate the extracellular reduction of Pu(V) and Cr(VI).[47,48] The involvement of saccharides in arsenate reduction was reaffirmed by the suppressed arsenate reduction by Au^{3+} (Figure 6a), which depleted the hemiacetal groups of reducing saccharides in EPS.[33] With the presence of 25 μM Au^{3+}, the reduction efficiency of arsenate was markedly decreased by 52.4%, and the k_{obs} decreased by 57.1% (values presented in Table S2).

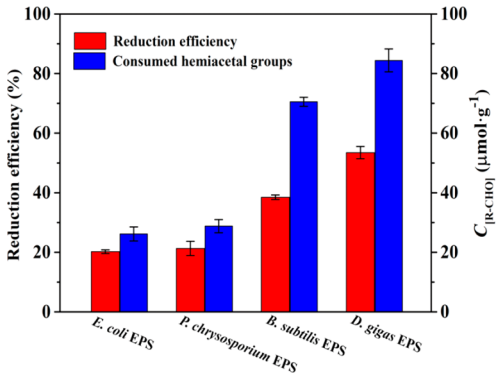

Figure 5. Reduction efficiency (%) of arsenate (initially at 40 $\mu g \cdot L^{-1}$) in aqueous dissolved EPS at the end of the reaction (72 h) and the consumption of hemiacetal groups as aldehyde equivalents ($C_{[R\text{-}CHO]}$, $\mu mol \cdot g^{-1}$) of EPS due to the reaction with arsenate. The tested EPS were *E. coli* EPS (90 $mg \cdot L^{-1}$), *B. subtilis* EPS (94 $mg \cdot L^{-1}$), *D. gigas* EPS (78 $mg \cdot L^{-1}$), and *P. chrysosporium* EPS (64 $mg \cdot L^{-1}$). Error bars for arsenate reduction efficiency represent standard deviations calculated from triplicate samples, and those for consumption of hemiacetal groups represent standard variations calculated from duplicate samples.

It is well-documented that quinoid-like structures in natural organic matter can act as electron shuttles and hence effectively catalyze biogeochemical redox reactions in the environment.[19,49,50] By this mechanism, the presence of humic substances can greatly accelerate the reduction of arsenate by *Shewanella oneidensis* MR-1.[19] The existence of humic-like substances in *B. subtills* EPS was verified by the EEM fluorescence signals at excitation/emission of 350/440 nm[39] (Figure S4). The role of quinone structures in arsenate reduction by EPS was revealed by the accelerated reaction kinetics by juglone (a model quinone compound) (Figure 6a). With the presence of 5.7 μM juglone, the reduction efficiency of arsenate was significantly increased by 38.4%, and the k_{obs} was increased by 71.2% (values presented in Table S2). No arsenate was reduced if only juglone was present (data not shown). Thus, the quinone structures in EPS can facilitate arsenate reduction resulting from the electron shuttling ability. Note the content of quinone moieties in the as-collected EPS was expected to be relatively low as the bacterial cells were subjected to repeated washing with water prior to EPS extraction which had presumably removed large portions of soluble quinone moieties. The presence of dissolved oxygen suppressed but not terminated arsenate reduction (Figure 6a), likely due to the competitive oxidation reaction with the reducing agents in EPS.

The reducing capability was also compared between bulk EPS of *B. subtilis* and the two separated molecular weight fractions, low-MW EPS (<3 kDa) and high-MW EPS (>3 kDa) (Figure 6b). Their size exclusion chromatograms are displayed in Figure S5. The contributions of the two molecular weight fractions to the overall arsenate reduction by bulk EPS were not proportional to their TOC contribution (63% of low-MW

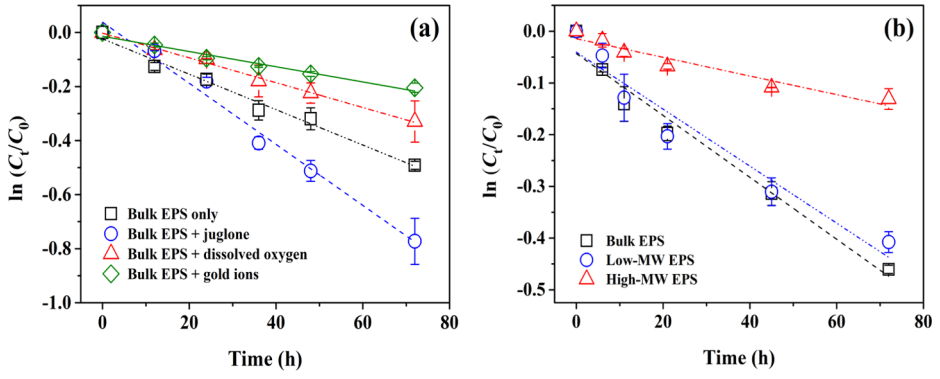

Figure 6. Pseudo-first-order kinetics of reduction of arsenate (initially at 10 $\mu g \cdot L^{-1}$) by *B. subtilis* EPS under different conditions plotted as ln(C_t/C_0) against time. (a) *B. subtilis* EPS (29.4 mg $C \cdot L^{-1}$) with and without the presence of gold ions (25.0 $\mu mol \cdot L^{-1}$), juglone (5.7 $\mu mol \cdot L^{-1}$), and dissolved oxygen (6.9 $mg \cdot L^{-1}$). (b) Different molecular weight fractions of *B. subtilis* EPS: bulk EPS (28.7 mg $C \cdot L^{-1}$), low-MW EPS (18.1 mg$C \cdot L^{-1}$), and high-MW EPS (9.8 mg $C \cdot L^{-1}$). Error bars represent standard deviations calculated from triplicate samples.

https://dx.doi.org/10.1021/acs.est.0c01186
Environ. Sci. Technol. 2020, 54, 6185−6193

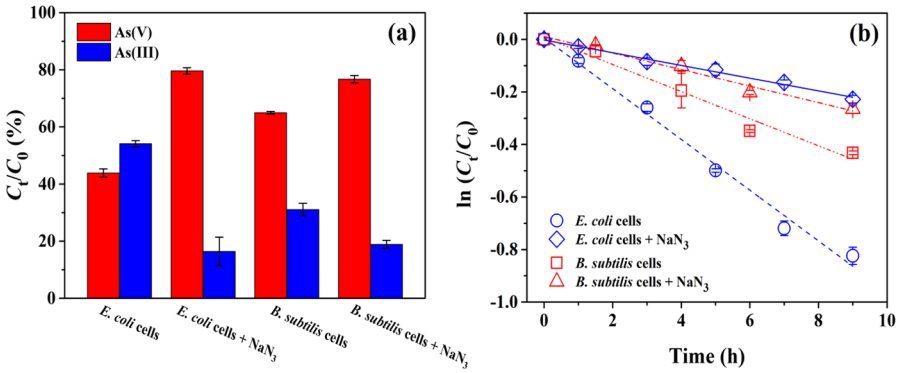

Figure 7. Reduction of arsenate (initially at 45 $\mu g \cdot L^{-1}$) to arsenite in aqueous suspension of *E. coli* (2.8×10^{12} cells·L^{-1}) or *B. subtilis* (3.0×10^{12} cells·L^{-1}) with and without the presence of (cytochrome-inhibitor) sodium azide (7.7 mM). Ratios of concentrations (C_t) of residual arsenate and arsenite (product) at the end of the reaction (9 h) to the initial concentration (C_0) of arsenate (a) and pseudo-first-order kinetics of reduction of arsenate plotted as $\ln(C_t/C_0)$ against time (b). Error bars represent standard deviations calculated from triplicate samples.

EPS and 34% of high-MW EPS). In fact, the arsenate reduction efficiency (32.6%) by low-MW EPS accounted for 88.4% of the arsenate reduction efficiency (36.9%) by bulk EPS. These results demonstrate that arsenate reduction by EPS was dominated by the low molecular weight (<3 kDa) components rather than by the high molecular weight (>3 kDa) components. These results also ruled out the possibility that arsenate reduction by the tested EPS was mainly driven by reduced proteins (including enzymes and cytochromes) due to their much higher molecular weights. Additionally, the k_{obs} values were $(6.0 \pm 0.5) \times 10^{-3}$ h^{-1} for bulk EPS, $(5.5 \pm 0.7) \times 10^{-3}$ h^{-1} for low-MW EPS, and $(1.8 \pm 0.2) \times 10^{-3}$ h^{-1} for high-MW EPS (Table S2). Obviously, the sum of the two k_{obs} values for low-MW EPS and high-MW EPS exceeded the k_{obs} value for bulk EPS. This was expected given that the anionic arsenate species had to surpass the interface energy barrier to reach and react with the active sites of reducing agents, which were likely harbored in (also) negatively charged structural components. Once normalized on TOC, the k_{obs} was ordered as low-MW EPS $[(3.0 \pm 0.4) \times 10^{-4}$ $(mgC \cdot h)^{-1}]$ > bulk EPS $[(2.1 \pm 0.2) \times 10^{-4}$ $(mgC \cdot h)^{-1}]$ > high-MW EPS $[(1.8 \pm 0.2) \times 10^{-4}$ $(mgC \cdot h)^{-1}]$, confirming the much higher reducing capability of low-MW EPS compared to high-MW EPS.

Mechanisms Proposed for Extracellular Arsenate Reduction. Although aqueous dissolved EPS alone were capable of reducing arsenate, intact EPS attached to cells pronouncedly hindered arsenate reduction. Specifically, bacterial reduction of arsenate was greatly facilitated by removing EPS from cells (Figure 1). On the other hand, knocking out the arsenic resistance genes (*arsB*, *arsC*, or both *arsB* and *arsC*) only moderately suppressed arsenate reduction. Furthermore, the resulting arsenite was detected mostly outside the bacterial cells (including the mutants Δ*arsB*, Δ*arsC*, and Δ*arsBC*). Therefore, extracellular reduction contributed significantly to the overall arsenate reduction by *E. coli* and *B. subtilis*. In addition to the reducing agents (reducing saccharides) and electron transfer mediators (quinones) in aqueous dissolved EPS, the cell outer membrane contains abundant redox-active proteins (cytochromes).[36,51] Previous studies have suggested that *c*-type cytochrome plays a key role in extracellular reduction of high-oxidation-state heavy metal oxyanions such as U(VI).[51,52]

To test the possible involvement of cytochromes, the reduction efficiency and the pseudo-first-order reaction kinetics of arsenate reduction by *E. coli* and *B. subtilis* cells were compared with and without the presence of NaN_3 (a cytochrome inhibitor) (Figure 7). The presence of NaN_3 (7.7 mM) greatly suppressed arsenate reduction with a larger extent observed for *E. coli*. The reduction efficiency decreased by 63.7% and 33.6% for *E. coli* and *B. subtilis*, respectively, and the k_{obs} decreased by 75.3% and 38.5% (Table S1). These results indicate that cytochromes were actively involved in bacterial arsenate reduction. Thus, the hindered arsenate reduction by intact EPS attached to cells could be explained by a barrier effect that decreases access to cytochromes in the cell outer membrane, in addition to decreased cell permeability. The larger extent of suppressed arsenate reduction by NaN_3 observed for *E. coli* relative to *B. subtilis* may be ascribed to their differently structured extracellular domains. Compared with Gram-negative *E. coli* cells, Gram-positive *B. subtilis* cells have a much thicker cell wall (10 to 80 nm) and lack a periplasm for hosting large-quantity extracellular cytochromes, and thus, the suppressing effect of NaN_3 was weaker. However, more work is warranted to elucidate the mechanism of arsenate reduction by reduced extracellular cytochromes, particularly the electron balance during the reaction process.

We herein propose the mechanisms for the extracellular reduction of arsenate by bacterial cells. First, with the aid of electron transfer mediators (e.g., quinones), the electron-donating agents (mainly reducing saccharides) in EPS can reduce arsenate to arsenite. Second, the reduced cytochromes in the extracellular matrix can reduce arsenate to arsenite. The electrons needed for the reduction of cytochromes are presumably donated by components in EPS (preferentially reducing sugars) eventually considering the absence of exogenous electron-donor substrates under the examined conditions. The relative importance of these two pathways is apparently dependent on the redox potential of the involved species as well as its mass transfer process within the extracellular matrix. As indicated by the enhanced reaction kinetics by the removal of EPS, cytochromes seemed to contribute more to the overall extracellular reduction of arsenate than reducing saccharides in EPS for the tested *E. coli* and *B. subtilis* cells.

Environmental Implications. Despite the large biomass fraction represented by EPS and their importance to microorganisms, how EPS affect the microbial redox transformation of arsenic is not well understood. This study first showed that arsenate reduction could be purely driven by the extracellular electron transfer of nonelectroactive common

https://dx.doi.org/10.1021/acs.est.0c01186
Environ. Sci. Technol. 2020, 54, 6185−6193

bacteria (*E. coli* or *B. subtilis*) or by aqueous dissolved EPS extracted from microorganisms alone. We further demonstrated that EPS acted as both reducing agent and permeability barrier in arsenate reduction by bacterial cells. Although the reduction efficiency of EPS is much lower compared to bacterial cells, the role of EPS in arsenate reduction in natural aquatic environments should not be overlooked in view of their abundance, ubiquity, and mobility. EPS account for up to 50% of the labile and semilabile dissolved organic matter in natural waters.[24−26] Overall, our study highlights the importance of microbial EPS in the toxicity, environmental fate, and biogeochemical cycle of redox-active heavy metals and semimetals.

■ ASSOCIATED CONTENT

Supporting Information

The Supporting Information is available free of charge at https://pubs.acs.org/doi/10.1021/acs.est.0c01186.

Tables S1 and S2, k_{obs} values for reduction of arsenate by bacterial cells or microbial EPS; Table S3, elemental compositions of the freeze-dried pristine *E. coli* EPS and *B. subtilis* EPS; Figure S1, mass distribution of arsenic species and pseudo-first-order kinetics in presence of pristine and low-EPS *B. subtilis* cells; Figure S2, reduction of arsenate to arsenite and mass balance as a function of time in presence of *B. subtilis* EPS; Figure S3, ratios of concentrations of residual arsenate and arsenite at end of reaction to initial concentration of arsenate for *E. coli* and its mutants (Δ*arsB*, Δ*arsC*, and Δ*arsBC*); Figure S4, EEM fluorescence spectra of *B. subtilis* EPS; and Figure S5, chromatograms of different molecular weight fractions of *B. subtilis* EPS (PDF)

■ AUTHOR INFORMATION

Corresponding Author

Dongqiang Zhu − *State Key Laboratory of Pollution Control and Resource Reuse, School of the Environment, Nanjing University, Jiangsu 210023, China; School of Urban and Environmental Sciences, Key Laboratory of the Ministry of Education for Earth Surface Processes, Peking University, Beijing 100871, China;* orcid.org/0000-0001-6190-5522; Phone: +86 (010) 62766405; Email: zhud@pku.edu.cn

Authors

Xinwei Zhou − *State Key Laboratory of Pollution Control and Resource Reuse, School of the Environment, Nanjing University, Jiangsu 210023, China*

Fuxing Kang − *College of Resources and Environmental Sciences, Nanjing Agricultural University, Jiangsu 210095, China;* orcid.org/0000-0001-9968-8367

Xiaolei Qu − *State Key Laboratory of Pollution Control and Resource Reuse, School of the Environment, Nanjing University, Jiangsu 210023, China;* orcid.org/0000-0002-9157-4274

Heyun Fu − *State Key Laboratory of Pollution Control and Resource Reuse, School of the Environment, Nanjing University, Jiangsu 210023, China;* orcid.org/0000-0002-0014-1829

Pedro J. J. Alvarez − *Department of Civil and Environmental Engineering, Rice University, Houston, Texas 77251, United States;* orcid.org/0000-0002-6725-7199

Shu Tao − *School of Urban and Environmental Sciences, Key Laboratory of the Ministry of Education for Earth Surface Processes, Peking University, Beijing 100871, China;* orcid.org/0000-0002-7374-7063

Complete contact information is available at: https://pubs.acs.org/10.1021/acs.est.0c01186

Notes

The authors declare no competing financial interest.

■ ACKNOWLEDGMENTS

This work was supported by the National Natural Science Foundation of China (Grants 41991331, 21920102002, and 21777002).

■ REFERENCES

(1) Bissen, M.; Frimmel, F. H. Arsenic-a review. part I: occurrence, toxicity, speciation, mobility. *Acta Hydrochim. Hydrobiol.* **2003**, *31* (1), 9−18.

(2) Nriagu, J. O.; Pacyna, J. M. Quantitative assessment of worldwide contamination of air, water and soils by trace metals. *Nature* **1988**, *333* (6169), 134−139.

(3) Duker, A. A.; Carranza, E. J. M.; Hale, M. Arsenic geochemistry and health. *Environ. Int.* **2005**, *31* (5), 631−641.

(4) Cullen, W. R.; Reimer, K. J. Arsenic speciation in the environment. *Chem. Rev.* **1989**, *89*, 713−764.

(5) Smedley, P. L.; Kinniburgh, D. G. A review of the source, behaviour and distribution of arsenic in natural waters. *Appl. Geochem.* **2002**, *17* (5), 517−568.

(6) Oremland, R. S.; Stolz, J. F. The ecology of arsenic. *Science* **2003**, *300* (5621), 939−944.

(7) Andreae, M. O. Distribution and speciation of arsenic in natural waters and some marine algae. *Deep-Sea Res.* **1978**, *25* (4), 391−402.

(8) Stolz, J. F.; Basu, P.; Santini, J. M.; Oremland, R. S. Arsenic and selenium in microbial metabolism. *Annu. Rev. Microbiol.* **2006**, *60*, 107−130.

(9) Zobrist, J.; Dowdle, P. R.; Davis, J. A.; Oremland, R. S. Mobilization of arsenite by dissimilatory reduction of adsorbed arsenate. *Environ. Sci. Technol.* **2000**, *34* (22), 4747−4753.

(10) Ahmann, D.; Krumholz, L. R.; Hemond, H.; Lovley, D. R.; Morel, F. M. M. Microbial mobilization of arsenic from sediments of the Aberjona Watershed. *Environ. Sci. Technol.* **1997**, *31* (10), 2923−2930.

(11) Jones, C. A.; Langner, H. W.; Anderson, K.; Mcdermott, T. R.; Inskeep, W. P. Rates of microbially mediated arsenate reduction and solubilization. *Soil. Sci. Soc. Am. J.* **2000**, *64* (2), 600−608.

(12) Macy, J. M.; Santini, J. M.; Pauling, B. V.; O'Neill, A. H.; Sly, L. I. Two new arsenate/sulfate-reducing bacteria: mechanisms of arsenate reduction. *Arch. Microbiol.* **2000**, *173* (1), 49−57.

(13) Newman, D. K.; Ahmann, D.; Morel, F. M. M. A brief review of microbial arsenate respiration. *Geomicrobiol. J.* **1998**, *15* (4), 255−268.

(14) Rosen, B. P. Biochemistry of arsenic detoxification. *FEBS Lett.* **2002**, *529* (1), 86−92.

(15) Dang, Y.; Walker, D. J. F.; Vautour, K. E.; Dixon, S.; Holmes, D. E. Arsenic detoxification by *Geobacter* species. *Appl. Environ. Microbiol.* **2017**, *83* (4), e02689-16.

(16) Stolz, J.; Basu, P.; Oremland, R. Microbial transformation of elements: the case of arsenic and selenium. *Int. Microbiol.* **2002**, *5* (4), 201−207.

(17) Corsini, A.; Cavalca, L.; Crippa, L.; Zaccheo, P.; Andreoni, V. Impact of glucose on microbial community of a soil containing pyrite cinders: role of bacteria in arsenic mobilization under submerged condition. *Soil Biol. Biochem.* **2010**, *42* (5), 699−707.

(18) Mukhopadhyay, R.; Rosen, B. P.; Phung, L. T.; Silver, S. Microbial arsenic: from geocycles to genes and enzymes. *FEMS Microbiol. Rev.* **2002**, *26* (3), 311−325.

(19) Qiao, J.; Li, X.; Li, F.; Liu, T.; Young, L. Y.; Huang, W.; Sun, K.; Tong, H.; Hu, M. Humic substances facilitate arsenic reduction and

release in flooded paddy soil. *Environ. Sci. Technol.* **2019**, *53* (9), 5034−5042.
(20) Yamamura, S.; Sudo, T.; Watanabe, M.; Tsuboi, S.; Soda, S.; Ike, M.; Amachi, S. Effect of extracellular electron shuttles on arsenic-mobilizing activities in soil microbial communities. *J. Hazard. Mater.* **2018**, *342*, 571−578.
(21) Jiang, J.; Bauer, I.; Paul, A.; Kappler, A. Arsenic redox changes by microbially and chemically formed semiquinone radicals and hydroquinones in a humic substance model quinone. *Environ. Sci. Technol.* **2009**, *43* (10), 3639−3645.
(22) Palmer, N. E.; Wandruszka, R. V. Humic acids as reducing agents: the involvement of quinoid moieties in arsenate reduction. *Environ. Sci. Pollut. Res.* **2010**, *17* (7), 1362−1370.
(23) Delnomdedieu, M.; Basti, M. M.; Otvos, J. D.; Thomas, D. J. Reduction and binding of arsenate and dimethylarsinate by glutathione: a magnetic resonance study. *Chem.-Biol. Interact.* **1994**, *90* (2), 139−155.
(24) Flemming, H. C.; Wingender, J. The biofilm matrix. *Nat. Rev. Microbiol.* **2010**, *8* (9), 623−633.
(25) Tourney, J.; Ngwenya, B. T. The role of bacterial extracellular polymeric substances in geomicrobiology. *Chem. Geol.* **2014**, *386*, 115−132.
(26) Bhaskar, P. V.; Bhosle, N. B. Microbial extracellular polymeric substances in marine biogeochemical processes. *Curr. Sci.* **2005**, *88* (1), 45−53.
(27) Braissant, O.; Decho, A. W.; Przekop, K. M.; Gallagher, K. L.; Glunk, C.; Dupraz, C.; Visscher, P. T. Characteristics and turnover of exopolymeric substances in a hypersaline microbial mat. *FEMS Microbiol. Ecol.* **2009**, *67* (2), 293−307.
(28) More, T. T.; Yadav, J. S. S.; Yan, S.; Tyagi, R. D.; Surampalli, R. Y. Extracellular polymeric substances of bacteria and their potential environmental applications. *J. Environ. Manage.* **2014**, *144*, 1−25.
(29) Li, S. W.; Sheng, G.; Cheng, Y. Y.; Yu, H. Q. Redox properties of extracellular polymeric substances (EPS) from electroactive bacteria. *Sci. Rep.* **2016**, *6* (1), 39098.
(30) Xiao, Y.; Zhang, E.; Zhang, J.; Dai, Y.; Yang, Z.; Christensen, H. E. M.; Ulstrup, J.; Zhao, F. Extracellular polymeric substances are transient media for microbial extracellular electron transfer. *Sci. Adv.* **2017**, *3* (7), No. e1700623.
(31) Xiao, Y.; Zhao, F. Electrochemical roles of extracellular polymeric substances in biofilms. *Curr. Opin. Electrochem.* **2017**, *4* (1), 206−211.
(32) Kang, F.; Alvarez, P. J.; Zhu, D. Microbial extracellular polymeric substances reduce Ag^{+} to silver nanoparticles and antagonize bactericidal activity. *Environ. Sci. Technol.* **2014**, *48* (1), 316−322.
(33) Kang, F.; Qu, X.; Alvarez, P. J.; Zhu, D. Extracellular saccharide-mediated reduction of Au^{3+} to gold nanoparticles: new insights for heavy metals biomineralization on microbial surfaces. *Environ. Sci. Technol.* **2017**, *51* (5), 2776−2785.
(34) Burton, K. A study of the conditions and mechanism of the diphenylamine reaction for the colorimetric estimation of deoxyribonucleic acid. *Biochem. J.* **1956**, *62* (2), 315−323.
(35) Kang, F.; Zhu, D. Abiotic reduction of 1,3-DNB by aqueous dissolved extracellular polymeric substances produced by microorganisms. *J. Environ. Qual.* **2013**, *42* (5), 1441−1448.
(36) Carlson, H. K.; Iavarone, A. T.; Gorur, A.; Yeo, B. S.; Tran, R.; Melnyk, R. A.; Mathies, R. A.; Auer, M.; Coates, J. D. Surface multiheme *c*-type cytochromes from *Thermincola potens* and implications for respiratory metal reduction by Gram-positive bacteria. *Proc. Natl. Acad. Sci. U. S. A.* **2012**, *109* (5), 1702−1707.
(37) Yang, T. Mechanism of nitrite inhibition of cellular respiration in *Pseudomonas aeruginosa*. *Curr. Microbiol.* **1985**, *12*, 35−39.
(38) Sun, G.; Williams, P. N.; Zhu, Y.; Deacon, C.; Carey, A. M.; Raab, A.; Feldmann, J.; Meharg, A. A. Survey of arsenic and its speciation in rice products such as breakfast cereals, rice crackers and Japanese rice condiments. *Environ. Int.* **2009**, *35* (3), 473−475.
(39) Zhu, L.; Qi, H.; Lv, M.; Kong, Y.; Yu, Y. W.; Xu, X. Component analysis of extracellular polymeric substances (EPS) during aerobic sludge granulation using FTIR and 3D-EEM technologies. *Bioresour. Technol.* **2012**, *124*, 455−459.
(40) Siggia, S.; Segal, E. Determination of aldehydes in presence of acids, ketones, acetals, and vinyl ethers. *Anal. Chem.* **1953**, *25* (4), 640−642.
(41) Lide, R. D. In *CRC handbook of chemistry and physics*, 84th, ed.; Electrochemical series, Vanýsek, P., Eds.; CRC Press: Boca Raton, 2004.
(42) Mukhopadhyay, R.; Rosen, B. P. Arsenate reductases in prokaryotes and eukaryotes. *Environ. Health Perspect.* **2002**, *110*, 745−748.
(43) Carlin, A.; Shi, W.; Dey, S.; Rosen, B. P. The *ars* operon of *Escherichia coli* confers arsenical and antimonial resistance. *J. Bacteriol.* **1995**, *177* (4), 981−986.
(44) Schmitt, J.; Flemming, H. C. FTIR-spectroscopy in microbial and material analysis. *Int. Biodeterior. Biodegrad.* **1998**, *41* (1), 1−11.
(45) Guo, J.; Zhang, X. Metal-ion interactions with sugars. The crystal structure and FTIR study of an $SrCl_2$-fructose complex. *Carbohydr. Res.* **2004**, *339* (8), 1421−1426.
(46) Kačuráková, M.; Capek, P.; Sasinková, V.; Wellner, N.; Ebringerová, A. FT-IR study of plant cell wall model compounds: pectic polysaccharides and hemicelluloses. *Carbohydr. Polym.* **2000**, *43* (2), 195−203.
(47) Harish, R.; Samuel, J.; Mishra, R.; Chandrasekaran, N.; Mukherjee, A. Bio-reduction of Cr(VI) by exopolysaccharides (EPS) from indigenous bacterial species of Sukinda chromite mine, India. *Biodegradation* **2012**, *23* (4), 487−496.
(48) Boggs, M. A.; Jiao, Y.; Dai, Z.; Zavarin, M.; Kersting, A. B. Interactions of plutonium with *Pseudomonas* sp. strain EPS-1W and its extracellular polymeric substances. *Appl. Environ. Microbiol.* **2016**, *82*, 7093−7101.
(49) Lovley, D. R.; Coates, J. D.; Blunt-Harris, E. L.; Phillips, E. J. P.; Woodward, J. C. Humic substances as electron acceptors for microbial respiration. *Nature* **1996**, *382*, 445−448.
(50) Klüpfel, L.; Piepenbrock, A.; Kappler, A.; Sander, M. Humic substances as fully regenerable electron acceptors in recurrently anoxic environments. *Nat. Geosci.* **2014**, *7*, 195−200.
(51) Marshall, M. J.; Beliaev, A. S.; Dohnalkova, A. C.; Kennedy, D. W.; Shi, L.; Wang, Z.; Boyanov, M. I.; Lai, B.; Kemner, K. M.; McLean, J. S.; Reed, S. B.; Culley, D. E.; Bailey, V. L.; Simonson, C. J.; Saffarini, D. A.; Romine, M. F.; Zachara, J. M.; Fredrickson, J. K. c-Type cytochrome-dependent formation of U(IV) nanoparticles by *Shewanella oneidensis*. *PLoS Biol.* **2006**, *4* (9), No. e268.
(52) Cao, B.; Ahmed, B.; Kennedy, D. W.; Wang, Z.; Shi, L.; Marshall, M. J.; Fredrickson, J. K.; Isern, N. G.; Majors, P. D.; Beyenal, H. Contribution of extracellular polymeric substances from *Shewanella* sp. HRCR-1 biofilms to U(VI) immobilization. *Environ. Sci. Technol.* **2011**, *45* (13), 5483−5490.

https://dx.doi.org/10.1021/acs.est.0c01186
Environ. Sci. Technol. 2020, 54, 6185−6193